LA-UR-04-2457

Approved for public release; distribution is unlimited.

Title: PLATE DAMAGE IDENTIFICATION USING WAVE PROPAGATION AND IMPEDANCE METHODS

Author(s): JEANNETTE R. WAIT, GYUHAE PARK, HOON SOHN, CHARLES R. FARRAR

Submitted to: SPIE'S 9TH INTERNATIONAL SYMPOSIUM ON NDE FOR HEALTH MONITORING AND DIAGNOSTICS, SAN DIEGO, CA, MARCH 15-18, 2004

Plate Damage Identification Using Wave Propagation and Impedance Methods

Jeannette R. Wait, Gyuhae Park, Hoon Sohn and Charles R. Farrar
Engineering Sciences and Applications – Weapons Response Group,
Los Alamos National Laboratory, Los Alamos NM, 87545;

ABSTRACT

This paper illustrates an integrated approach for identifying structural damage in an aluminum plate. Piezoelectric (PZT) materials are used to actuate/sense the dynamic response of the structure. Two damage identification techniques are integrated in this study, including Lamb wave propagations and impedance methods. In Lamb wave propagations, one PZT launches an elastic wave through the structure, and responses are measured by an array of PZT sensors. The changes in both wave attenuation and reflection are used to detect and locate the damage. The impedance method monitors the variations in structural mechanical impedance, which is coupled with the electrical impedance of the PZT. Both methods operate in high frequency ranges at which there are measurable changes in structural responses even for incipient damage such as small cracks or loose connections. This paper summarizes two methods used for damage identification, experimental procedures, and additional issues that can be used as a guideline for future investigations.

Keywords: Damage detection, structural health monitoring, piezoelectric (PZT) materials, Lamb waves, impedance method, active sensing systems

1. INTRODUCTION

Piezoelectric materials are very useful in structural health monitoring because they can perform both duties of sensing and actuation within a local area of the structure. The molecular structure of PZT materials produces a coupling between the electrical and mechanical domains. Therefore, this type of material generates mechanical strain in response to an applied electric field. Conversely, the materials produce electric charges when stressed mechanically. This coupling property allows one to design and deploy an "*active*" and "*local*" sensing system whereby the structure in question is locally excited by a known input, and the corresponding responses are measured by the same excitation source. Some advantages of these devices are: compactness, light-weight, low-power consumption, ease of integration into critical structural areas, ease of activation through electrical signals, higher operating frequency, and low cost. The employment of a known input also facilitates subsequent signal processing of the measured output data. Examples of documented success using PZTs in the areas of active and local sensing are Lamb wave propagations (Kessler, 2002) and the impedance-based structural health monitoring methods (Park, 2003) which are both currently being investigated at Los Alamos National Laboratory (LANL).

This paper illustrates damage identification processes in a plate structure based on both Lamb wave propagation and self-sensing impedance methods. In particular, the Lamb wave propagation method has been used for identifying simulated surface cracks and the impedance method has been used for detecting joint connection damage in a clamped condition. The integration procedure is somewhat straightforward because the same PZT patches can be used for both methods. The main focus of this research is the capability of the sensing system to detect incipient and evolving damage in real-time before serious damage has developed, which is the most important function of structural health monitoring.

2. METHODOLOGY

2.1. Impedance Method

The process to be used with the impedance-based monitoring technique uses both the direct and converse version of the piezoelectric effect simultaneously to obtain an impedance signature for the structure. When a PZT patch is driven by a fixed, alternating electric field, a small deformation is produced in the PZT wafer and the attached structure. The subsequent response to the mechanical vibration is transferred back to the PZT wafer in the form of an electrical response. When damage causes the mechanical dynamic response to change, it is manifested in the electrical response of the PZT wafer. The electrical impedance, which is the ratio of the input voltage to the output current, is related to the structural impedance through the following equation (Sun, 1995):

$$Y(\omega) = \frac{I}{V} = i\omega a \left(\bar{\varepsilon}_{33}^{\ T} - \frac{Z_s(\omega)}{Z_s(\omega) + Z_a(\omega)} d_{3x}^2 \hat{Y}_{xx}^{\ E} \right) \tag{1}$$

In equation (8), Y is the electrical admittance (inverse of impedance), Z_a and Z_s are the PZT's and the structure's mechanical impedances, respectively, $Y_{xx}^{\ E}$ is the complex Young's modulus of the PZT with zero electric field, d_{3x} is the piezoelectric coupling constant in the arbitrary x direction at zero stress, $\varepsilon_{33}^{\ T}$ is the dielectric constant at zero stress, and a is a geometric constant of the PZT. When a structure becomes damaged, the mechanical impedance is altered by changes in the structural stiffness and/or damping. Because all other variables in equation (1) are determined only by the PZT properties, only the external structure's impedance, Z_s, uniquely determines the overall electrical impedance of the PZT. Therefore, a change in the electrical impedance is regarded as an indication that the structure has been damaged. The impedance-based method is shown to be excellent at localizing damage because input to the structure is generally greater than 30 kHz, which limits the dynamic response of the structure to the local area of the PZT patch. For more information on current impedance-based structural health monitoring (SHM) methods, consult (Park, (2000a, 2001, 2003), Giurgiutiu, 2002).

2.2. Lamb Wave Propagation

Since the 1960s, the ultrasonic research community has studied Lamb waves for the nondestructive evaluation of plates (Bourasseau, 2000). Lamb waves are mechanical waves corresponding to vibration modes of plates with a thickness on the same order of magnitude as the wavelength. Because Lamb waves travel long distances and can be applied with conformable PZT actuators/sensors that require little power, they are suitable for online structural health monitoring. The advances in sensor and hardware technologies for efficient generation and detection of Lamb waves and the need to detect sub-surface damage in laminate composites structures, particularly those used in aircraft industries, has led to a significant increase in the studies that use Lamb waves for detecting defects in structures.

The dispersive nature of Lamb waves means that the different frequency components of the Lamb waves travel at different speeds and that the shape of the wave packet changes as it propagates through solid media. There are two types of modes that form when exciting a structure with Lamb waves: asymmetric and symmetric. The asymmetrical modes are analogous to shear waves (equivalent to S waves in earthquake engineering), while symmetrical modes are analogous to compression waves (equivalent to P waves in earthquake engineering).

The type of damage that can be detected using Lamb waves depends on which mode, A_0 or S_0, is excited. The symmetric mode is sensitive to through-thickness irregularities such as embedded delamination and through-cracks, whereas the asymmetric mode is sensitive to surface anomalies and is therefore often used to detect surface cracks and surface delamination. For damage detection applications, it may be useful to limit the number of generated Lamb waves to two fundamental modes, namely the S_0 and A_0 modes, and to select a less dispersive frequency region so that the interpretation of response signals becomes easier. To obtain only S_0 or A_0 modes, the frequency of the Lamb wave must be below the range of the other modes. The S_0 mode exhibits dispersive behavior as it travels through a material, but it tends to attenuate faster than the A_0 mode. The first asymmetric Lamb wave (A_0 mode), however, can propagate long distances with little dispersion, and no higher modes are present to clutter the resulting response waves.

The first step in designing the input frequency is to compute the dispersion curve of the group velocities for a structure. The velocities of asymmetric and symmetric waves are computed from the following equations (Kessler, 2002).

$$V_{asymmetric} = \sqrt{(\lambda + 2G)/\rho}, \quad V_{symmetric} = \sqrt{G/\rho},$$
$$G = \frac{E}{2(1+\nu)}, \qquad \lambda = \frac{\nu E}{(1-2\nu)(1+\nu)} \tag{2}$$

where E is the effective Young's modulus, G is the shear modulus, ν is the Poisson ratio, and ρ is the material density. Once the velocities of asymmetric and symmetric waves are calculated, the dispersion curve shown in Figure 1 (only shows S_0 and A_0 modes) is obtained by finding the Lamb wave solution for the wave equation (Kessler, 2002 and Vallen Systeme, 2003). This dispersion curve is used to initially determine a frequency range where only the fundamental modes propagate and to find any non-dispersive regions. While the input frequency should be high enough to make the wavelength of the Lamb wave comparable to the scale of local damage, the driving frequency also needs to be low enough so that higher modes are not in the same frequency range as the fundamental symmetric (S_0) and asymmetric (A_0) modes. Note that the dispersion curve is only used as a guideline, and several trial-and-error experiments are conducted to tune the optimal driving frequency value.

The shape of the Lamb wave pulse also plays a significant role. The most widely used wave is a fixed frequency burst, which is a sine wave with a Gaussian window as specified in Equation (3) (Lin, 2001)

$$A = \frac{1}{2}\sin\omega t\left[1 - \cos\left(\frac{\omega t}{n}\right)\right]. \tag{3}$$
$$\omega = 2\pi f, \quad n = \#of\ peaks$$

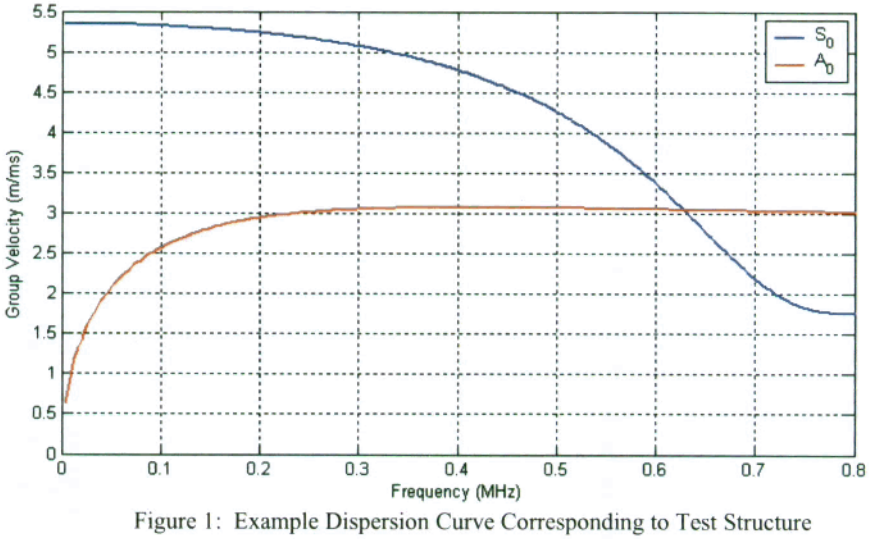

Figure 1: Example Dispersion Curve Corresponding to Test Structure

Additionally, applying a larger voltage at the desired driving frequency produces a stronger Lamb wave and the wavespeed calculation is more accurate (Kessler, 2002). Also, a larger driving voltage provides more energy and an increased signal to noise ratio, but requires more power.

The optimal frequency of a Lamb wave is one that produces a response signal with a large separation between the arrival of the S_0 and A_0 modes. This separation ensures that the mode of interest, S_0, can be distinguished from any other modes such as A_0 or S_1. Based on the dispersion curve in Figure 1, the recommended shape of an input wave, and the separation of modes, the optimal input frequency was determined to be a 300 kHz windowed sine function with 4 cycles.

Several methods have been proposed to enhance the interpretation of the measured Lamb wave signals to detect and locate structural damage. They are based on changes in wave attenuations using wavelets (Kessler, 2002; Sohn 2004), time-frequency analysis (Lin et al 2001), wave reflections (Giurgiutiu 2002, Lemistre and Balageas 2001), and time of arrival information (Kessler 2002). In this analysis, the wave attenuation feature is first used to locate the region of the suspected damaged area, and then, the pulse-echo analysis (wave reflections) is used to locate the damage site.

3. TEST STRUCTURE & EXPERIMENTAL PROCEDURES

The structure tested is a cantilevered aluminum plate. The test structure is shown in Figure 2. The aluminum plate is 101-cm x 10-cm x 3-mm-thick. Four holes, 1.35-cm in diameter, at one end of the plate allow it to be clamped, in a cantilevered condition, to unistrut columns using two 6.5-cm x 6.5-cm x 6.35-mm-thick x 20.32-cm-long steel angles. The unistrut columns are bolted to an aluminum base plate (3.8-cm x 1.4-cm x 1.4-cm) and all bolted connections are tightened to a torque of 16.9-Nm (150-in-lb) for all tests.

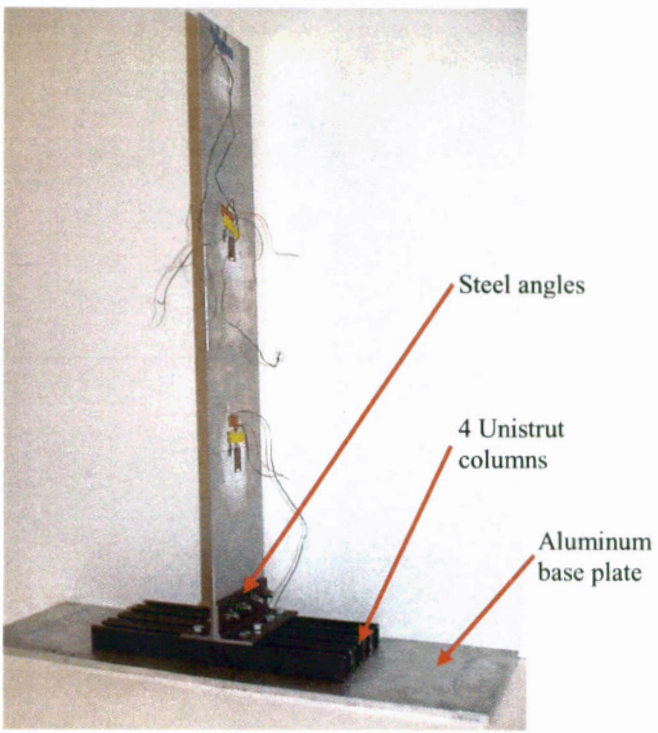

Figure 2: Test Structure

The cantilevered aluminum plate is instrumented with 4 PZT patches and 2 Macro-Fiber Composite (MFC) patches. The locations of these actuators/sensors are shown in Figure 3 (a-d). These actuators/sensors were mounted on the aluminum plate with super glue and then immediately vacuumed bagged for a day to create a uniform bond between the plate and actuators/sensors. Lead wires were soldered to the PZT patches after the vacuum bagging process was complete. Ideally, only 3 patches are required for the wave propagation analysis. However, because of equipment limitations, i.e. the same PZT cannot be used as a sensor and an actuator simultaneously for the pulse-echo method; another PZT patch was installed directly beside a PZT or MFC, to measure any wave reflections that may occur at the actuation location.

Two different data acquisition systems are used to collect data from the test structure. For the Lamb wave method, a commercially available portable PC is used to send a 300 kHz windowed sine function with 4 peaks (Figure 4) to a designated actuator (P1, P2, P3, P4, M1 or M2). The system then records the responses of the different actuator-sensor pairs under test. A different portable data acquisition system (Agilent 4294A, Impedance analyzer) is used to collect data for the impedance method. The same actuator-sensor pairs as for the Lamb wave method are investigated for the impedance method. Table 1 shows the different actuator-sensor pairs for the Lamb wave and impedance methods.

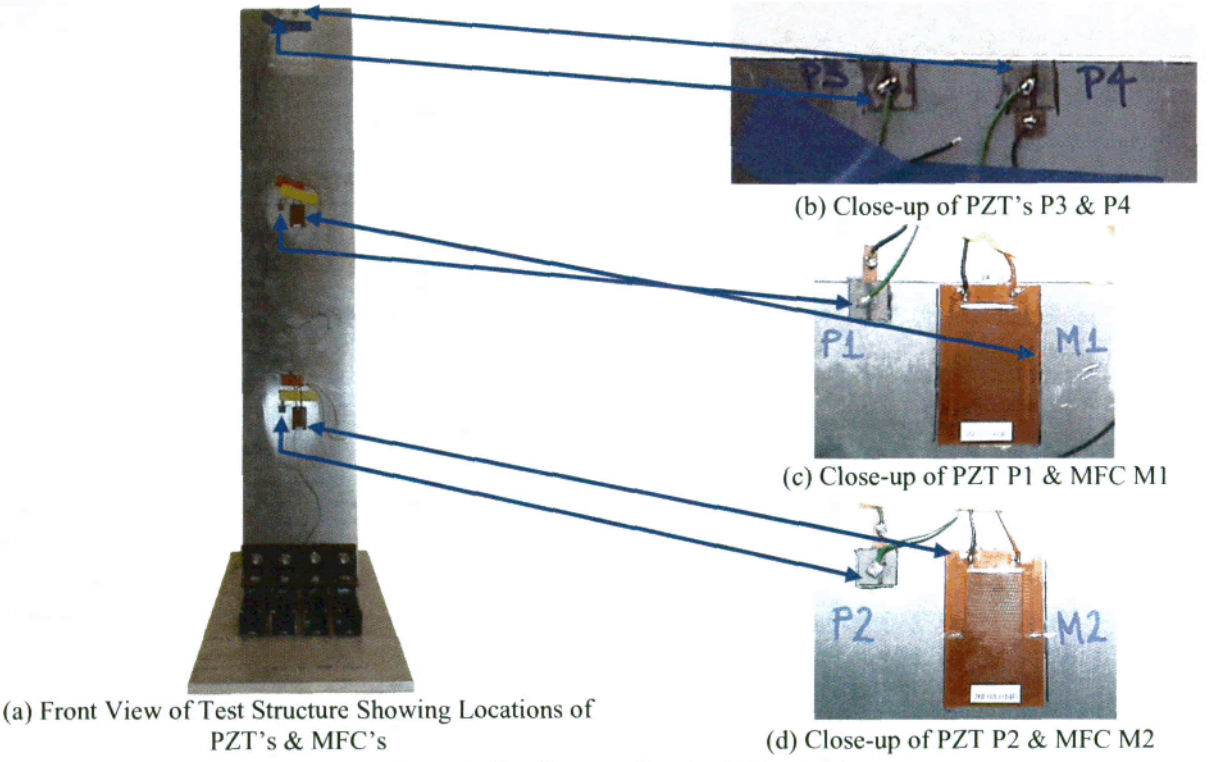

(a) Front View of Test Structure Showing Locations of PZT's & MFC's

(b) Close-up of PZT's P3 & P4

(c) Close-up of PZT P1 & MFC M1

(d) Close-up of PZT P2 & MFC M2

Figure 3: Test Structure Showing PZT & MFC Locations

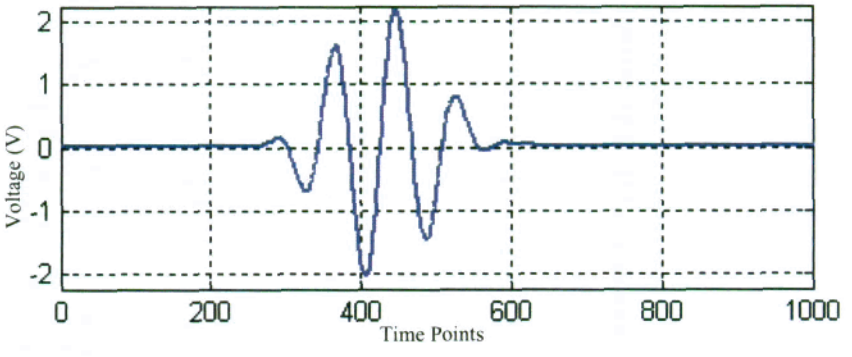

Figure 4: Example Lamb Wave Input Excitation

Table 1: Actuator-Sensors Pairs for Lamb Wave and Impedance Methods

Actuator	Sensors
P1	P2, P3, P4, M1, M2
P2	P1, P3, P4, M1, M2
P3	P1, P2, P4, M1, M2

Several damage cases are investigated this research. Simulated damage is introduced to the cantilevered plate by clamping a pair of small blocks (4-cm x 1.5-cm x 1.5-cm) to the plate with a c-clamp (one on the front side of the plate and one on the back side of the plate that lined up with the block on the front side). Clamping the blocks to the plate simulates changes in the flexural/extensional stiffness and the inertia of the plate in a localized area. Although it is not "real" damage, the process allows multiple tests to be performed with several different configurations. Two of the results are presented here. The first damage is introduced between P3 and P1 (Damage 1) as shown in Figure 5 (a). Then the pair of blocks is placed between P1 and P2 (Figure 5 (b)), as the second damage case. Before the simulated damage is initiated in the plate, several baseline data sets (corresponding to those in Table 1) are acquired in order to

establish undamaged threshold limits. For each damage case, the blocks are held in place while the c-clamp is hand-tightened. After the blocks are secured in place and the plate stops oscillating, the same data sets as the baseline tests are recorded. Each data set for all actuator-sensor pairs (baseline and damage cases) is repeated five times. All data are then post-processed with the algorithms developed at LANL for the Lamb wave propagation method.

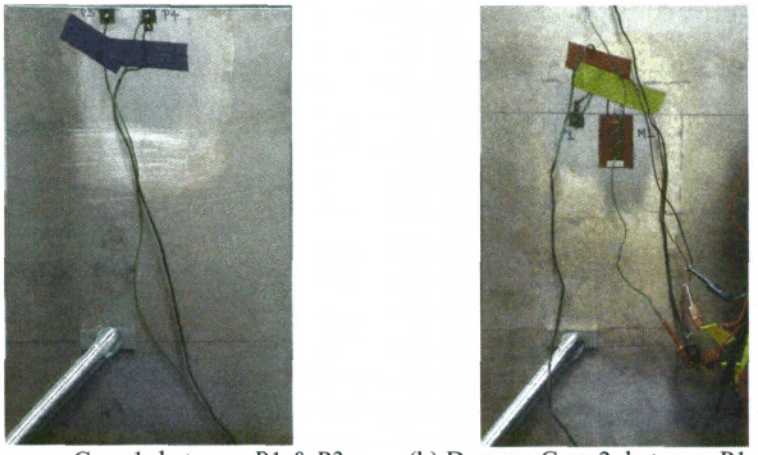

(a) Damage Case 1: between P1 & P3 (b) Damage Case 2: between P1 & P2

Figure 5: Two Damage Cases Introduced to Aluminum Plate

The impedance analysis was not performed for damage cases 1 and 2 because the relatively large mass increased the affect of the simulated cracks (weight of blocks and C-clamp). There were several distinct changes found in the impedance signatures before and during the simulated damage, but the changes may not be solely caused by the simulated cracks. The changes in the signatures are most likely influenced by the relatively large weight of the C-clamp. Actual, physical, surface cracks will be introduced in future experiments and the impedance method will then be used to assess the condition of the test structure. There is, however, ample evidence that the impedance methods can detect and locate surface damage by tracking the high frequency impedance changes (Park et al 2003). In this research, the impedance method is used to identify damage in the clamped-end (bolted cantilever connection). Damage is introduced by loosening one of the bolts through the two steel angles. Data are then collected for both the Lamb wave and impedance methods (as described above).

4. RESULTS

4.1. Simulated Cracks

The Lamb wave propagation of ten baselines, with P1 as an actuator and M1 as a sensor (which can be considered as co-location), and the actuator-sensor pair of P1 and P2, with the first arrival of the S_0 mode, are shown in Figure 6. The arrival time for both S_0 and A_0 is measured to be approximately 5-m/ms, and 3.4-m/ms respectively, which is close to the analytical prediction. Because of the relatively small size of the structure, the reflected waves from the boundaries are observed, which make the pulse-echo analysis quite difficult. The reflections come mainly from the boundaries, which are perpendicular to the wave path. The MFC patches can be used to alleviate the problem associated with the boundary reflection because of their unidirectional sensing capability. However, as can be seen in the Figure 6, the MFC can still measure the waves coming from the vertical direction with a somewhat distorted shape.

The principle of the pulse-echo analysis is that the damage (or discontinuity) produces diffracted waves, referred to as "a mode conversion process" (Han et al. 1999), which create new (reflected) waves depending on the angle of incidence. Both S_0 and A_0 modes can be created by this process. In this study, only the reflected S_0 modes are tracked because they travel much faster than the A_0 mode. The problem associated with the boundary-reflected waves becomes more significant: if the boundary-reflected waves are out-of-phase with the damage-reflected waves, the result is attenuation instead of increased amplitude in the combined measured reflected waves. Therefore, in this analysis, the first

occurrence of changes in waves (of both attenuation and increase) is considered as a damage indication. This is based on the assumption that there always exists the direct wave path between the damage (simulated crack) and the actuator.

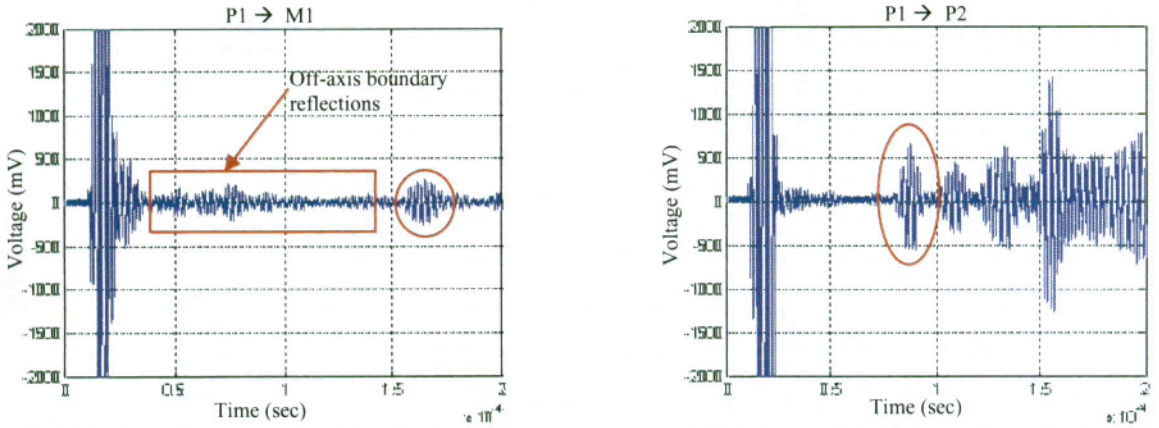

(a) M1 Sensor Response to Actuation by P1 (b) P2 Sensor Response to Actuation by P1

Figure 6: Baseline Measurements from Different Actuator-Sensor Pairs (red circles indicated first arrival of S_0 mode)

As a first step, the wave attenuation between P1 and P3, P1 and P2, and between P2 and the clamped boundary are recorded. The changes in each path are considered as the presence of damage in the corresponding region. Once the damaged region is identified, the location of the simulated crack is inversely identified by tracking the time of flight of the reflected wave from the actuator location, similar to processes used for triangulation procedures. For damage case 1, there is large attenuation in the path between P1 and P3, while no changes are observed in any other actuator-sensor pairs. The result indicates that the region between P1 and P3 contains the damage, as shown in Figure 7 (a) and (b). Once the damaged region is identified, the pulse-echo analysis is performed to locate the damaged site. For this process, the time-frequency analysis was performed on baseline and test cases. Analyzing time and frequency components simultaneously produces a clearer indication of the arrival of the reflected waves. In the time frequency analysis, changes in the power spectral density (PSD) corresponding to 300 kHz, which is the input frequency, are recorded as a function of time. The algebraic difference between the test and baseline PSDs are processed with the time-frequency analysis. The first arrival of the reflected wave causes a change in the magnitude of the PSD. As can be seen in Figure 8 (a), the first reflected wave for the actuator-sensor pair, P1 and M1 (co-location), occurs at $5.5e^{-5}$ seconds (the actuation was initiated at $1e^{-5}$-seconds), which indicates that the damage is located around 0.13-m (($5.5e^{-5}$-seconds/2) x $5e^{3}$-m/s) from the sensor. Another analysis is performed for the P2 and P1 combination (distance from sensor = [(1.3 e^{-4}-sec - 0.8 e^{-4}-sec)/2] x $5e^{3}$-m/s = 0.10-m), as shown in Figure 8 (b) and for the path between P3 and P4 d = 0.25-m. From these three actuator-sensor pairs, the damage was located using a modified triangularization procedure (see Figure 9).

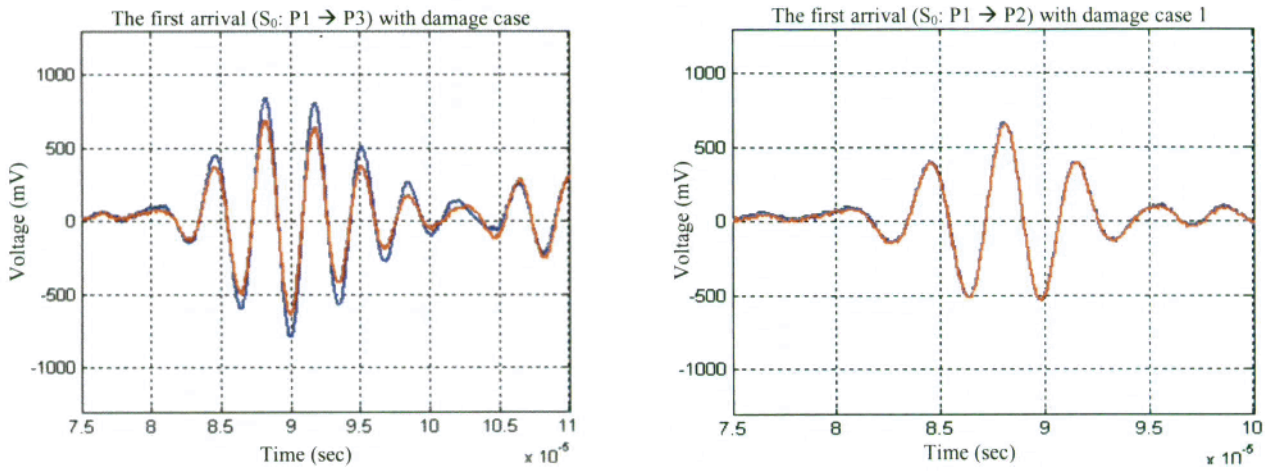

(a) P3 Sensor Response to Actuation by P1 (b) P2 Sensor Response to Actuation by P1

Figure 7: The First Arrival of A_0 modes (blue = baseline, red = damage case 1)

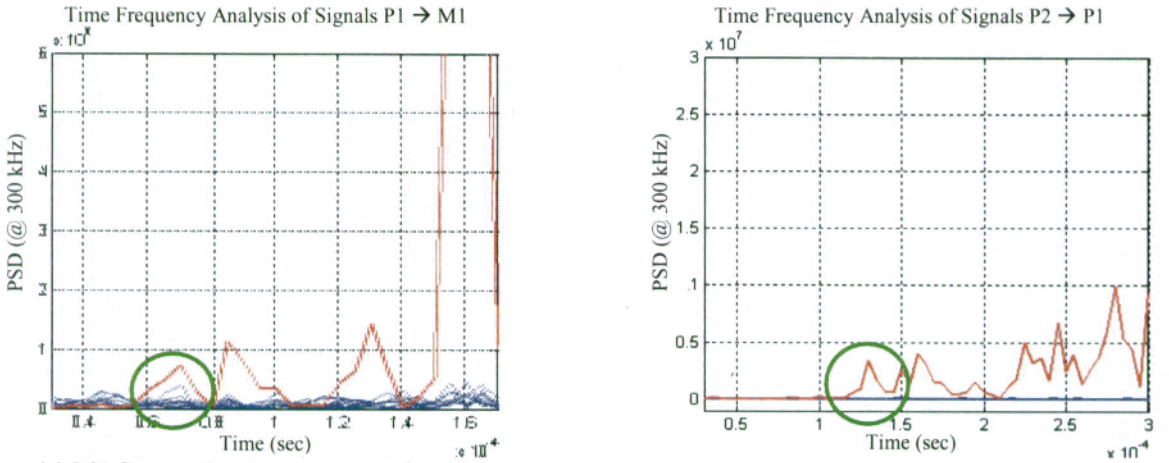

(a) M1 Sensor Response to Actuation by P1 (b) P2 Sensor Response to Actuation by P1

Figure 8: Time-Frequency Analysis (300 kHz). The First Reflection Indicates the Location of Damage (green circles)

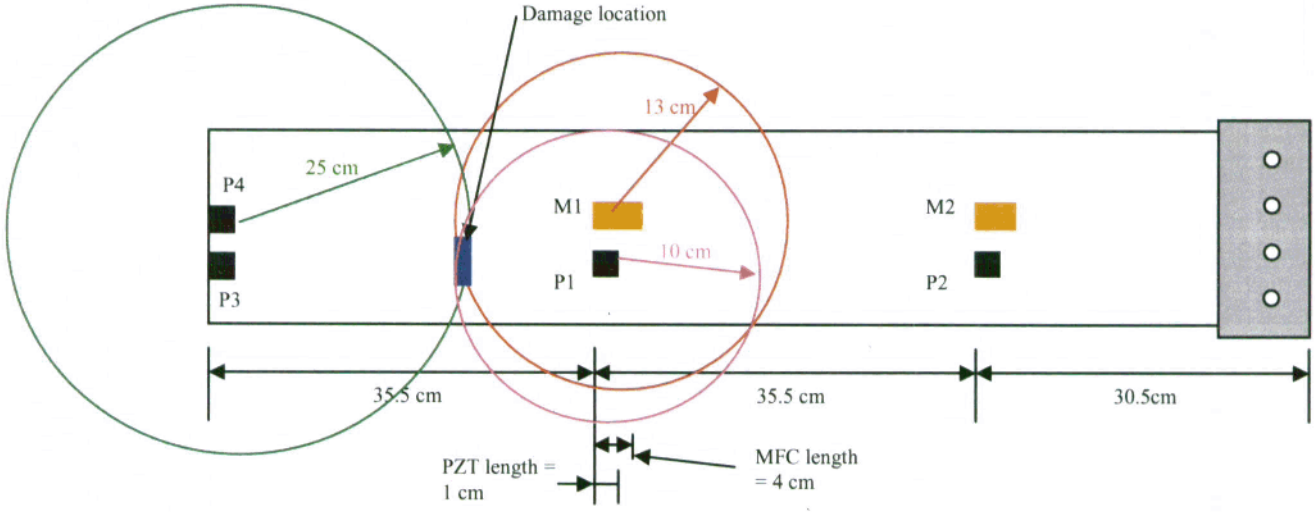

Figure 9: Damage Location Process for Damage Case 1

Similar results were for observed in damage Case 2. The first arrival of the S_0 mode shows a significant attenuation in the region between P1 and P2. Again, the suspected area is identified by using time-frequency analysis of each path. Figure 10 shows the wave attenuation, time-frequency analysis, and damage localization process for damage case 2.

In most cases, the detection and localization of damage was successful. However, there are a few cases that the proposed method fails to locate damage. First, if the damage is located too close to the sensor/actuator, the reflected waves are easily mixed with the (electromagnetic) actuation signals making the localization difficult. In addition, if the block is placed parallel to the length of the plate and the wave propagation path, it produces relatively small attenuation or reflection. Furthermore, the existence of the boundary reflected waves makes it complicated to identify and to distinguish the "damage" reflected waves. Ideally, the pulse-echo analysis should be performed before the first boundary reflected wave arrives back at the actuator. Nevertheless, the combined use of the features associated with wave attenuation and reflection enables the detection and location of damage with fewer sensors/actuator combinations compared to methods based on only one feature. The advantage will be more significant, if the method is combined with the impedance methods for the crack identification process, because the impedance method is most sensitive to the near-field damage, and not affected by any changes that occur in the far-field.

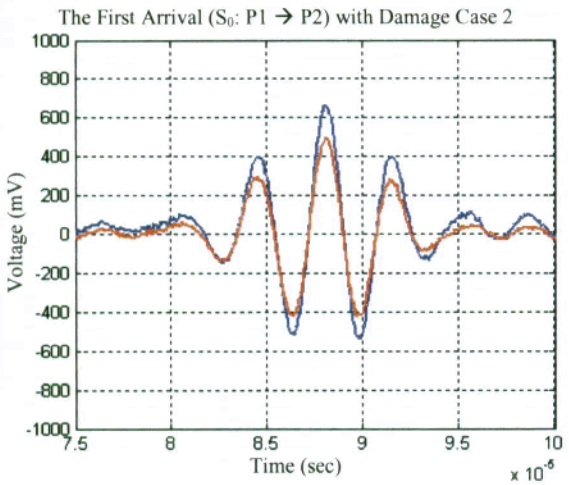

(a) P2 Sensor Response to Actuation by P1

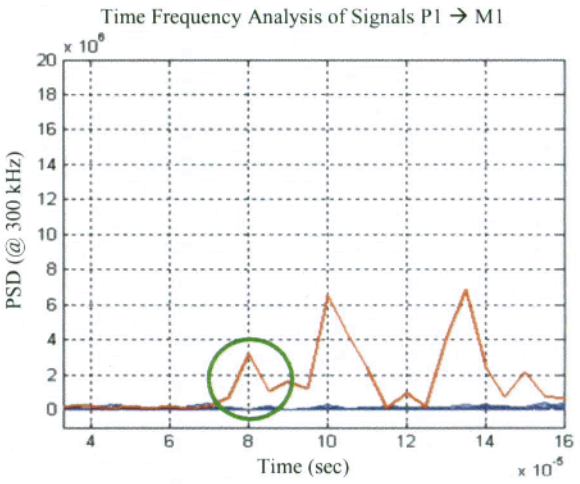

(b) M1 Sensor Response to Actuation by P1

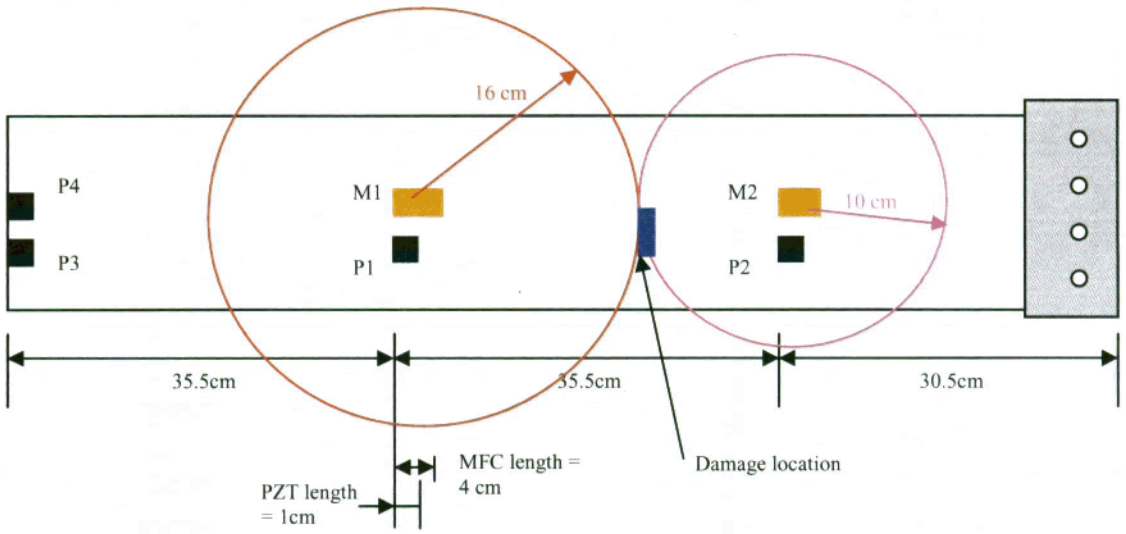

Figure 10: Damage Localization Process for Damage Case 2

4.2. Connection-Type Damage

The next experiments include identifying connection damage using impedance methods. This type of damage is introduced by loosening one of the connection bolts in the clamped end of the test structure. The impedance (real part) of P2, in the frequency range of 100-105 kHz, is shown in Figure 11 with two different damage conditions. Only the real portion of the electrical impedance is analyzed to predict damage because it is more sensitive to structural changes than the imaginary part. For damage case 1, the bolt torque is reduced to 8.5-Nm (75 in-lb) (from 16.9-Nm (150 in-lb)). Damage case 2 refers the condition where the same bolt has been loosened to 1.1-Nm (10 in-lb). It can be seen from the figures that, with an increasing level of damage, the impedance signature shows a relatively large change in shape and it clearly indicates imminent damage. For the first level of damage, only a small variation along the original signal (undamaged curve) is observed. This is because the first level of damage can be categorized as the incipient stage. When the bolt is loosened to a torque of 1.1-Nm (10 in-lb), the impedance signature shows more pronounced variations as compared to previous readings; i.e. new peaks and valleys appear in the entire frequency range. This change occurs because the loosened bolt modifies the apparent stiffness and damping of the joint. This variation shows the extreme sensitivity of the impedance-based method to the presence of connection-type damage in the structure.

A damage metric chart is illustrated in Figure 12. In this analysis, correlation coefficients (CC) are used to compare the baselines and damage test cases. Figure 12 illustrates the value corresponding to (1-CC), in which damage shows up

with an increased value of 0 to 1. The first five measurements are made when no damage is present (i.e. baseline conditions). Tests 6 and 7 correspond to damage case 1, and tests 8 and 9 correspond to damage case 2. The damage metric chart is constructed after each measurement has been taken in order to give some indication of the conditions of a structure through comparison with a reference measurement. As can be seen in the figure, the baselines are repeatable, and when damage is introduced, there is an increase in the damage metric values. This correlation chart provides a quick insight into the extent of damage and provides a quantitative comparison between different data sets. Although the impedance method cannot precisely predict the exact nature and size of the damage, the method provides somewhat quantitative information about the condition of a structure by showing an increasing damage metric with increased severity of damage.

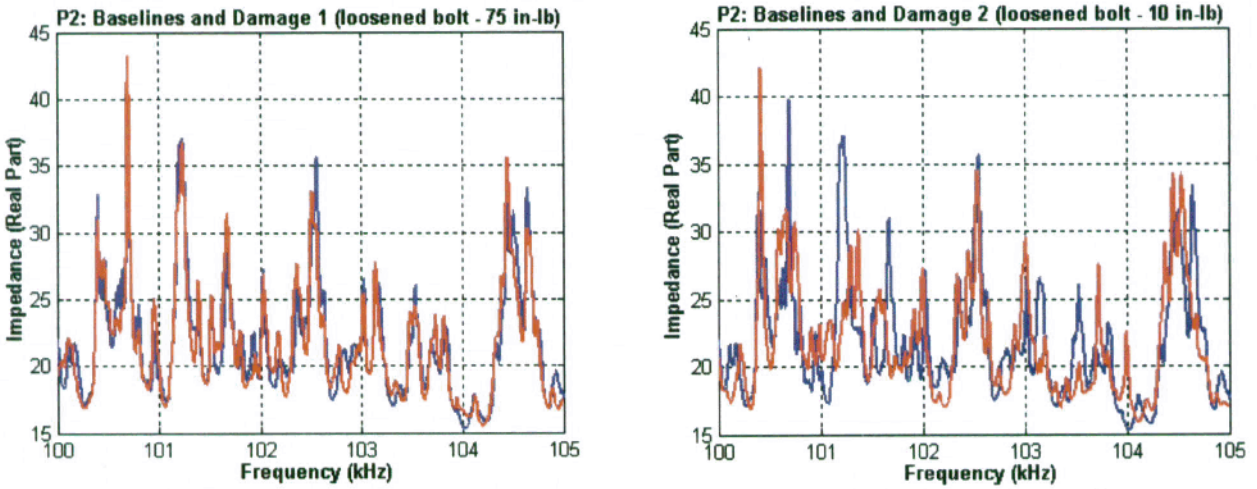

Figure 11: The Impedance (Real Part) Measurement for P2 for Two Connection-type Damage Cases

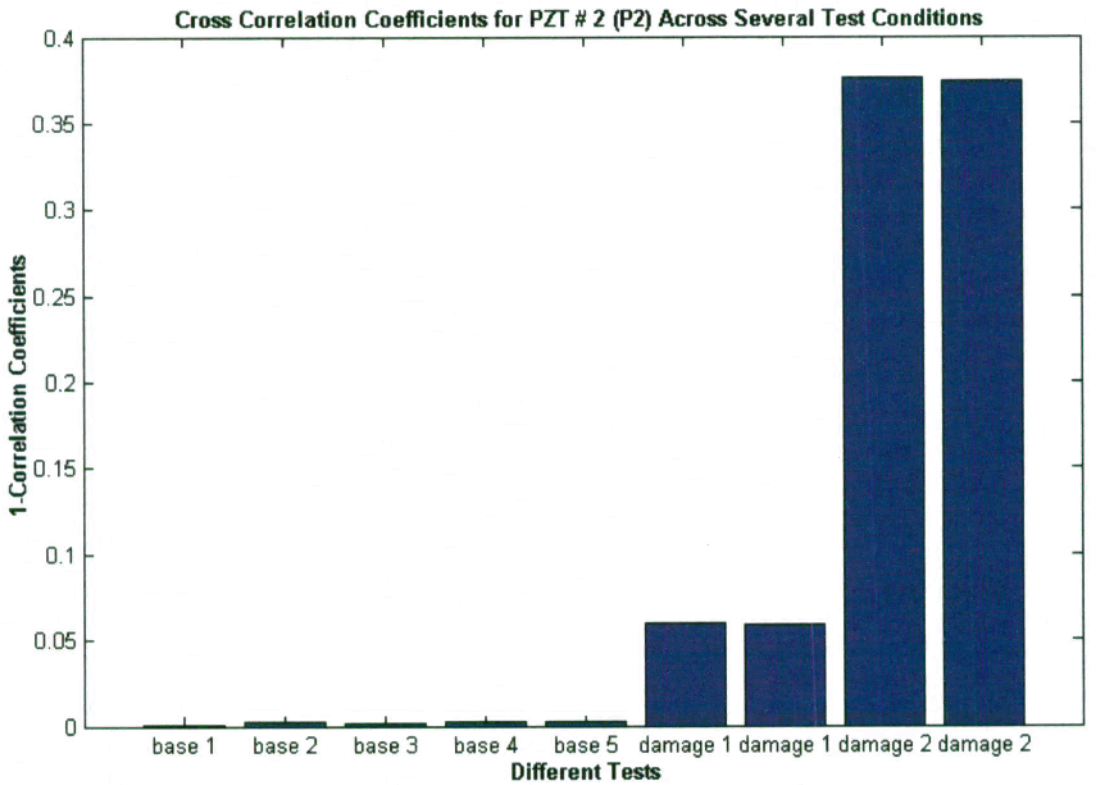

Figure 12: Cross Correlation Damage Metric Chart

An attempt is also made to use the Lamb wave technique to locate the connection-type damage. But, the changes in Lamb wave propagations, particularly in the reflected wave from the clamped joint, were not clearly identifiable because, even after loosening the bolt, almost the same amount of waves (before and after the induced damage) are reflected from the end of the plate and holes (used for bolt connections). On the other hand, for the impedance-based method, P3 shows about the same sensitivity to the connection damage as P2. In other words, the damage was not localized in the given frequency ranges. This might be because either the effect of the damage is on the global scale or the frequency range is far too low for damage localization. However, by observing no change in wave propagations, one can infer that the changes in the impedance signature indicate connection-type damage.

5. DISCUSSION

The combined use of PZT patches for identifying plate damage has been presented. While the method shows great potential, certain issues must be addressed to handle real-world applications. The impedance methods will be integrated into the plate damage identification process. The integration will make the damage localization much easier as confirmed by previous studies. The damage considered in this study (simulated crack) is not realistic and the performance of the proposed method must be verified with real damage. The use of wavelet analysis, instead of using the time-frequency analysis will certainly provide advantages for this method, because there is a tradeoff between time and frequency resolution in the time-frequency analysis. In addition, the threshold limit should be well established to properly classify the arrival of the reflected waves for the pulse-echo analysis. In this study, by mixing the use of MFCs and PZTs, the threshold limits were established for each PZT/MFC combination, which is quite problematical. Furthermore, the presence of the boundary-reflected wave makes the pulse-echo analysis quite complicated and the optimization of sensor/actuator deployment must be addressed. Finally, the automated process in signal processing for more complex geometry should be developed. All of the issues mentioned above are currently being investigated at LANL.

6.CONCLUSIONS

An integrated approach for identifying structural damage in an aluminum plate has been presented. In this study, piezoelectric materials are used to actuate/sense the dynamic response of the structure with the Lamb wave propagation and impedance methods. As illustrated in the examples presented in this research, the impedance measurements are made using the same PZT actuators/sensors used for Lamb wave propagations. For the Lamb wave propagation, both wave attenuation and reflection information are utilized to detect and locate simulated through-cracks in the structure. The impedance methods are used to detect connection-type damage, in which the wave propagation method is less sensitive. The proposed method was verified with experiments using an aluminum plate with a clamped end. Several issues are outlined that can be used as a guideline for future investigations.

ACKNOWLEDGMENTS

This research is funded through the Laboratory Directed Research and Development program at Los Alamos National Laboratories.

REFERENCES

[1] Bourasseau, N., Moulin, E., Delebarre, C., and Bonniau, P. (2000), "Radome Health Monitoring with Lamb Waves: Experimental Approach," *NDT&E International,* Vol. 33, pp. 393-400.

[2] Giurgiutiu, V, Zagrai, A. and Bao J.J. (2002), "Piezoelectric Wafer Embedded Active Sensors for Aging Aircraft Structural Health Monitoring," *International Journal of Structural Health Monitoring*, 1, pp. 41-61.

[3] Han J B, Cheng J C, Wang T H and Bertelot Y 1999 Mode analysis of laser generated transient ultrasonic Lamb waveforms in composite plate by wavelet transform *Material Evaluation* pp 837–840

[4] Kessler, S.S. (2002), *Piezoelectric-based In-situ Damage Detection of Composite Materials for Structural Health Monitoring Systems,* Ph.D. Dissertation, MIT, Massachusetts.

[5] Lemistre, M., Balageas, D. (2001), "Structural Health Monitoring System based on Diffracted Lamb Wave Analysis by Multiresolution Processing," *Smart Materials and Structures*, Vol. 10, pp. 504-511.
[6] Lin, M., Qing, X., Kumar, A., Beard, S. (2001), "Smart Layer and Smart Suitcase for Structural Health Monitoring Applications," *Proceedings of SPIE*, Vol. 4332, pp. 98-106.
[7] Park, G., Cudney, H., and Inman, D.J. (2001), "Feasibility of Using Impedance-based Damage Assessment for Pipeline Systems," *Earthquake Engineering & Structural Dynamics Journal*, Vol. 30, No. 10, pp. 1463-1474.
[8] Park, G., Cudney, H., Inman, D.J. (2000a), "Impedance-based Health Monitoring of Civil Structural Components," *ASCE Journal of Infrastructure Systems*, Vol. 6, No. 4, pp. 153-160.
[9] Park, G., Sohn, H., Farrar, C.R., and Inman, D.J. (2003), "Overview of Piezoelectric Impedance-based Health Monitoring and Path Forward," *The Shock and Vibration Digest,* Vol. 35, No. 6, pp. 451-463.
[10] Sohn, H., Park, G., Wait, J.R., Limback, N.P., Farrar, C.R. 2004. "Wavelet-based Signal Processing for Detecting Delamination in Composite Plates," *Smart Materials and Structures*, Vol. 13, No. 1, pp. 153-160.
[11] Sun, F., Chaudhry, Z., Liang, C., and Rogers, C.A. (1995), "Truss Structure Integrity Identification Using PZT Sensor-Actuator," *Journal of Intelligent Material Systems and Structure,* V.6, pp. 134-139.
[12] Vallen Systeme (2003), "Vallen System: The Acoustic Emission Company," http://www.vallen.de/.